

# AUTOMATION OF SAMPLE IDENTIFICATION FOR NEUTRON BEAMLINES

A. Chen, J. Einstein-Curtis, M. Henderson, J. P. Edelen\*, RadiaSoft LLC, Boulder, CO, USA  
B. Krishna, C. Hoffmann, G. Taufer, S. Calder  
Oak Ridge National Laboratory, Oak Ridge, TN, USA

## Abstract

Neutron scattering experiments are a critical tool for the investigation of molecular structure in compounds. The HB-2A neutron powder diffractometer at the High Flux Isotope Reactor at ORNL conducts magnetic studies of samples by illuminating them with different energy neutron beams and recording the scattered neutrons. Proper identification and alignment of the sample during an experiment is key to ensuring high quality data is collected. At present, this process is performed manually by beamline scientists. RadiaSoft, in collaboration with the beamline scientists and engineers at ORNL, has developed a machine learning-based software automating sample identification. We utilize a fully connected convolutional neural network configured in a U-Net architecture to identify the sample and its center of mass. We then move the sample using a custom Python-based EPICS IOC interfaced with the motors. In this paper, we provide an overview of our machine learning tools and show our results identifying samples at ORNL.

## INTRODUCTION

Automation of alignment processes for accelerators and accelerator users is broad area of research. For example, recent work from NSLS-II has focused on the application of different Bayesian optimization approaches for alignment for x-ray beamlines [1, 2]. Additionally, RadiaSoft has been engaged in a multi-year collaboration to utilize machine learning for sample identification, noise reduction [3], and alignment [4]. While work on alignment automation and testing has largely focused on the TOPAZ single crystal diffractometer, recent studies have shown success for sample alignment using the neutron camera at HB-2A.

The HB-2A beamline is primarily used for magnetic structure determination [5] and permits the application of high external fields and pressure, and services many ultra-low temperature experiments. Figure 1 shows a picture of the diffractometer end station. The constant wavelength and simple profile of its neutron beam, along with its relatively low noise environment, allows for interchangeable sample environments on HB-2A with minimal calibration. The beamline also features a variety of sample changing options that allow multiple samples to be loaded per session to increase throughput.

There are several challenges associated with sample alignment at HB-2A. The two primary challenges are that the sample is not visible when it is not illuminated by the beam.

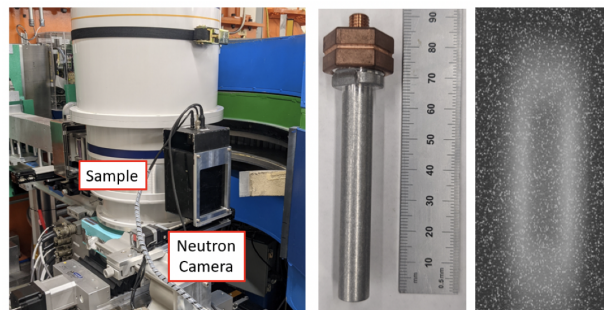


Figure 1: The HB-2A powder neutron diffractometer. Left: the sample and detector area. Center: a standard sample holder (in millimeters). Right: an example of a neutron image, with the powder sample appearing as a shadow-like image in the white beam.

Additionally, the presence of multiple samples necessitates precise positioning of the sample combined with slit closure to prevent from illuminating more than one sample at a time. Moreover, the use of neutron cameras for positioning relies on the ability to accurately identify the sample even when the signal to noise ratio is low. Each of these issues present challenges for control. While human operators are adept at sample identification, automation of this process is necessary to streamline the operation of the beamline.

In previous work we have utilized operator based image contouring to establish a ground truth for training ML based sample identification models. While effective, this requires beam-time to develop a training dataset and an operator to label images which is error prone and time consuming. As an alternative we have developed a generalized model of the HB-2A system that allows us to consider an object that is illuminated by the neutron beam and then generate a simulated neutron camera image. In this paper we will review our simulation tools, provide an analysis of model training using the new dataset, and then model testing on experimental data and compare the predicted sample center with the operator identified sample center.

## SIMULATION TOOLS

We built a simulator that creates a beam using a super-gaussian distribution that allows us to shape the profile to be more akin to a uniform beam with smooth edges. The sample then absorbs some of the beam casting a shadow, a parameter that can be modulated depending on the type of sample in question. Slits were also integrated into the simulation to enable full replication of the experimental setup at HB-2A.

\* jedelen@radiasoft.net

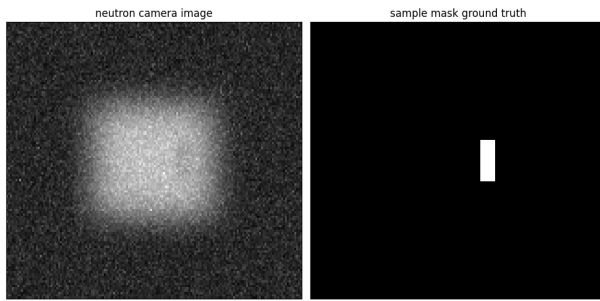


Figure 2: Example input image and output mask used for training.

Our framework is flexible and allows for the inclusion of multiple samples. Figure 2 shows an example image and the associated mask that can be used to train sample detection models and control agents.

## MODEL LEARNING

We trained a U-Net model using the simulation data and tested the model on both simulation data and experimental data from HB-2A. We chose a typical U-Net architecture, Fig. 3 as it is particularly well-suited to the extraction of spatial contextual information. This is due to its use of “skip connections” (hidden vector concatenations) between the contraction or encoding and expansion or decoding sides of the network structure. The training dataset used for our U-Net models contained 540 pairs of images and ground truth masks from our simulator. We trained models with 5 convolutional layers and 32 base filters. Our U-Net structure is similar to a typical image segmentation model, but it is more specialized in distinguishing a sample from surrounding noise.

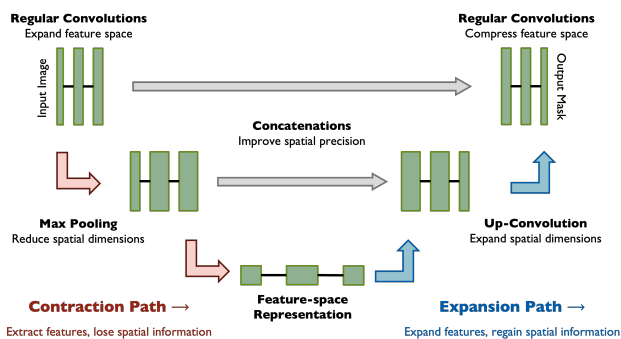


Figure 3: A diagram of the basic construction of a UNet CNN for image segmentation.

## TRANSFER ANALYSIS

We performed a transfer comparison between our existing models trained on expert labeled measurement data and the new models trained on the simulation data. Models trained on HB-2A data (Fig. 4) were presented with 534 pairs of images and masks, while models trained on simulated data were given 540 pairs. Tables 1 and 2 show the RMS error in sample center of mass prediction, in pixels, for each type of U-Net model trained, assuming a uniform sample density.

Table 1: Predicted RMS error for a model trained on different datasets and tested using images from the simulated beamline.

Training Data	Training Epochs	Single U-Net Error	U-Net Ensemble Error
HB-2A	100	8	6
Simulated	100	1	1
Simulated	250	1	1
Simulated	1000	1	1

Table 2: Predicted RMS error for a model trained on different datasets and tested using images from the HB-2A beamline.

Training Data	Training Epochs	Single U-Net Error	U-Net Ensemble Error
HB-2A	100	1	1
Simulated	100	4	3
Simulated	250	3	3
Simulated	1000	8	6

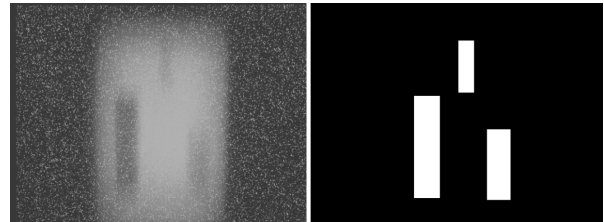


Figure 4: Neutron camera image of multiple samples at HB-2A (left) and corresponding UNet mask (right).

When tested on images taken by the HB-2A neutron camera, models trained on HB-2A data had high accuracy. Models trained on simulated data showed similar accuracy when trained for fewer epochs while accuracy degrades with longer training times.

An example of a sample prediction from a model trained on simulated data is shown in Fig. 5. As the number of training epochs increased, models trained on simulated data struggled to generalize to the HB-2A beamline. Sample prediction using images from the simulated beamline (Fig. 6) showed similar accuracy to the HB-2A data.

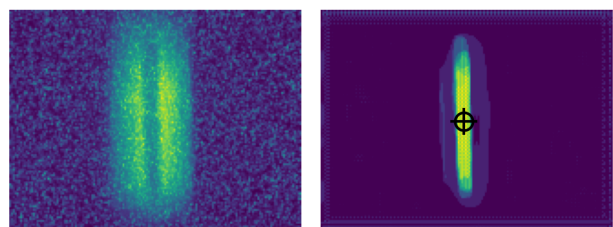


Figure 5: U-Net center of mass prediction on HB-2A data.

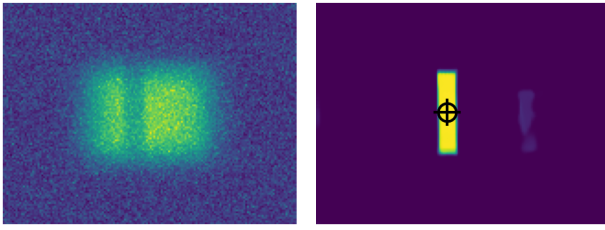


Figure 6: U-Net center of mass prediction on simulated data.

## CONCLUSIONS

Our beamline simulation is effective in training U-Net models with a comparable accuracy to models trained on neutron camera data directly from the HB-2A diffractometer. This simulation training data allows for larger dataset generation without necessitating beam-time. The use of U-Net models for sample identification presents an opportunity to streamline beam operations at HB-2A, without sacrificing data quality.

## ACKNOWLEDGMENTS

This work is supported in part by the U.S. Department of Energy, Office of Science, Office of Basic Energy Sciences, SBIR and STTR Program under Award Number(s) DE-SC0021555.

## REFERENCES

- [1] T. W. Morris *et al.*, “A general bayesian algorithm for the autonomous alignment of beamlines”, *Sync. Radiat.*, vol. 31, no. 6, pp. 1446–1456, 2024.  
doi:10.1107/S1600577524008993
- [2] T. W. Morris *et al.*, “Latent Bayesian optimization for the autonomous alignment of synchrotron beamlines”, in *Adv. Comput. Methods for X-Ray Opt. VI*, p. 126970B, 2023.  
doi:10.1117/12.2677895
- [3] I. Pogorelov *et al.*, “Machine Learning Based Noise Reduction of Neutron Camera Images at ORNL”, in *Proc. 19th Int. Conf. Accel. Large Exp. Phys. Control Syst. (ICALEPCS'23)*, Cape Town, South Africa, pp. 841–845, 2024.  
doi:10.18429/JACoW-ICALEPCS2023-TUPDP114
- [4] M. Henderson *et al.*, in *Proc. 19th Int. Conf. Accel. Large Exp. Phys. Control Syst. (ICALEPCS'23)*, Cape Town, South Africa, pp. 851–855, 2024.  
doi:10.18429/JACoW-ICALEPCS2023-TUPDP116
- [5] S. Calder *et al.*, “A suite-level review of the neutron powder diffraction instruments at oak ridge national laboratory”, *Rev. Sci. Instrum.*, vol. 89, no. 9, p. 092 701, 2018.  
doi:10.1063/1.5033906